Exergo-Economic and Environmental Analysis of a Solar Integrated Thermo-Electric Storage

(Article begins on next page)

23 April 2024

Article

Exergo-Economic and Environmental Analysis of a Solar Integrated Thermo-Electric Storage

Daniele Fiaschi [1] [ID], Giampaolo Manfrida [1] [ID], Karolina Petela [2,*] [ID], Federico Rossi [1,3], Adalgisa Sinicropi [3,4,5] [ID] and Lorenzo Talluri [1,*] [ID]

[1] Department of Industrial Engineering, University of Florence, 50134 Florence, Italy; daniele.fiaschi@unifi.it (D.F.); giampaolo.manfrida@unifi.it (G.M.); fe.rossi@unifi.it (F.R.)
[2] Department of Thermal Technology, Silesian University of Technology, Konarskiego 22, 44-100 Gliwice, Poland
[3] Department of Biotechnology, R2ES Lab, Chemistry and Pharmacy, University of Siena, Via A. Moro, 2, 53100 Siena, Italy; adalgisa.sinicropi@unisi.it
[4] CSGI, Center for Colloid and Surface Science, via della Lastruccia 3, 50019 Sesto Fiorentino, Italy
[5] Institute of Chemistry of Organometallic Compounds (CNR-ICCOM), Via Madonna del Piano 10, 50019 Sesto Fiorentino, Italy
* Correspondence: karolina.petela@polsl.pl (K.P.); lorenzo.talluri@unifi.it (L.T.)

Abstract: Renewable energies are often subject to stochastic resources and daily cycles. Energy storage systems are consequently applied to provide a solution for the mismatch between power production possibility and its utilization period. In this study, a solar integrated thermo-electric energy storage (S-TEES) is analyzed both from an economic and environmental point of view. The analyzed power plant with energy storage includes three main cycles, a supercritical CO_2 power cycle, a heat pump and a refrigeration cycle, indirectly connected by sensible heat storages. The hot reservoir is pressurized water at 120/160 °C, while the cold reservoir is a mixture of water and ethylene glycol, maintained at −10/−20 °C. Additionally, the power cycle's evaporator section rests on a solar-heated intermediate temperature (95/40 °C) heat reservoir. Exergo-economic and exergo-environmental analyses are performed to identify the most critical components of the system and to obtain the levelized cost of electricity (LCOE), as well as the environmental indicators of the system. Both economic and environmental analyses revealed that solar energy converting devices are burdened with the highest impact indicators. According to the results of exergo-economic analysis, it turned out that average annual LCOE of S-TEES can be more than two times higher than the regular electricity prices. However, the true features of the S-TEES system should be only fully assessed if the economic results are balanced with environmental analysis. Life cycle assessment (LCA) revealed that the proposed S-TEES system has about two times lower environmental impact than referential hydrogen storage systems compared in the study.

Keywords: energy storage; exergo-economic; exergo-environmental; solar energy; TEES; LCA

1. Introduction

The correct management of electric grids is being challenged by the widespread utilization of renewable energy sources (RES) [1]. This is due to the unsteady behavior of the variable renewable energies (VREs), which have the characteristic of being highly stochastic (wind), or dependent on daily cycles (solar). At present, the problem is approached with several measures, and among the others, energy storage represents an option that will certainly need to be used to support high market penetration of RES. Several energy storage systems are present in the market, from pumped-storage hydroelectricity to flywheel storage (FS), batteries, compressed or liquid

air energy storage (CAES/LAES), or chemical storage [2]. Each solution holds specific performance characteristics, which favors or hinders the selection of one technology over the other. Specifically, the most important selection criteria are the cost of the system, the total efficiency, the energy density, and the power rating. Table 1 presents the state of the art of the current studied storage technologies compared to the proposed solution of thermo-electric energy storage.

Table 1. Technological characteristics of energy storage systems [3–11].

Technology	Total Efficiency	Power Rating	Energy Density	Capital Cost (€/kWh)	Lifetime	Maturity
PHS	70–85%	200 MW–2 GW	Moderate	500–1500	>40 yr.	Mature
CAES/LAES	60–70%	10–300 MW	Medium	400–1200	>30 yr.	Early Commercial
CHS	35%	10 MW–1 GWh	Very High	900	>10 yr.	Demo
Flywheel	≥90%	1–20 MW	Medium-High	500–2000	20,000–100,000 cycles	Early Commercial
Li-ion batteries	85–95%	<10 MW	Very High	1000–3000	1000–10,000 cycles	Early Commercial
Lead—acid batteries	70–80%	<10 MW	High	500–1500	500–10,000 cycles	Mature
Super conductors	>90%	100 kW–5 MW	Medium-High	100–500	500,000 cycles	Demo
TEES	55–70%	100 kW–300 MW	Medium-High	500–2000	>25 yr.	Demo

Pumped storage technology is the most widespread one, and it has already been fully exploited, particularly in Europe [3]. The power range which it covers is quite wide and ranges from a few hundred MWs to a few GWs with total round-trip efficiencies in the span of 70–80%. The energy density of this technology is not very high, as it requires very big reservoirs, even if the capital cost is relatively low. Compressed air energy storage is one the preferred solution in short term scenario, as it guarantees a flexible configuration, and allows efficiency up to 70%. The power range is one order of magnitude below the pumped hydro storage (PHS), and it spans between 10 to 300 MWs. Liquid air energy storage can be examined as a CAES system with increased energy density. CAES and LAES systems have much higher energy density compared to PHS. [4] The main advantage of the flywheel storage system is the high storage density and the high response to charge and discharge cycles. Another main feature is the very high efficiencies that can be reached, over 90%, while the main issues are the relatively low lifetime (<100,000 cycles) and the high cost per kW installed. The power range of this technology is between 1 and 20 MW [5]. Several types of batteries are utilized as energy storages, but the most common ones are lead-acid and lithium-ion ones. The main trait of batteries is the very high energy intensity, coupled with a high roundtrip efficiency. The main drawbacks of batteries are the low lifetime, the high cost and the very high environmental impact [6]. In the last years, superconducting magnetic energy storage has been studied, as it guarantees very high conversion efficiency (>90%), with relatively high-power density. The Power range for this technology is between 10 kW and 5 MW. The capital cost of this technology is moderate [3,7].

Among the other technologies, thermo-electric energy storage (TEES) allows being utilized in a wide range of operation, giving, therefore, a suitable solution to the dispatch ability issue [12], without incurring in the intrinsic drawbacks of pumped-storage hydroelectricity [13], which is bound to geographical constraints, or batteries, having a limited lifetime [14] and raising problems in the end-of-life management.

The basic configuration of a TEES system is the one including a power cycle, which works between two temperature levels, fixed through the utilization of storage tanks, a heat pump and a refrigeration cycle, which maintain the temperature levels of the storages. The power cycle may be either a trans-critical CO_2 cycle [15,16] or a Brayton cycle [17,18]. Supercritical CO_2 cycles have recently found a widespread interest both in the research and the industrial world. Particularly, in [19], an extensive review of the architecture, the components, and the optimal cycle condition is carried out. The TEES solution has been mainly proposed for large electrical energy storage, using sensible heat hot rocks for the high-temperature heat storage; this can indeed be an attractive solution for large utilities and grid operators, as a substitute or in support of pumped hydro.

In [4] it was shown that multi-MW TEES could achieve roundtrip efficiency close to 70%, for complex investigated configuration of the cycles, while utilizing the simplest solution only a 50%

efficiency was reached. Furthermore, they presented a valuable model for the dimensioning of ground heat exchangers, which are often used in TEES applications as hot storage tanks. Furthermore, in [5] a thermo-economic optimization of the TEES system with transcritical CO_2 cycles was carried out. The main result was the complex optimization which provided, for the assessed case a roundtrip efficiency of about 65% for the system to be economically viable. Another exergo-economic analysis was carried out in [20], where a marginal round trip efficiency of 72% was found, and LCOE of 0.49 €/kWh was obtained for a hundred kW TEES configuration.

Therefore, when comparing TEES storage systems, to other technologies, it emerges that it is not the most outstanding one regarding cost and efficiency, however, it has several assets, such as its flexible configuration, no geographical constraints, relatively long lifetime and, when compared to other storage technologies (e.g., batteries), also a lower environmental impact.

Thermo-electric energy storage (TEES) systems utilizing solar energy to increase the storage roundtrip efficiency are scarcely studied in the literature [21], especially from an environmental point of view. Therefore, the exergy, exergo-economic and exergo-environmental analyses of a solar-assisted TEES system are proposed in the present study to investigate the possibility of developing a multi-functional energy storage system, capable to provide electricity, heat and/or cold at a reasonable cost and with attractive environmental performance. The current proposal addresses much lower power ranges (100–200 kWe peak) compared to the literature and energy storages in the range from 100 to 300 kWh, capable to serve the daily needs of small communities largely relying on photovoltaics (20–50 kWe peak) for their energy supply (typical southern Europe or African countries climate conditions), with a special focus on environmental performance. This is because—in recent years—environmental issues are becoming increasingly pressing, and an economic analysis alone can no longer provide sufficient indications to guarantee the attractiveness and feasibility of a plant.

Several types of environmental impact assessment methods are commonly applied to energy storage systems as these technologies aim to improve the environmental sustainability of energy and electric systems. Among these, life cycle assessment (LCA) is one of the most commonly used as it allows to analyze all the phases of the lifecycle of a technology. An interesting overview of studies focusing on the application of LCA to energy storage systems is provided in [22], where the eco-profile of photovoltaic systems assisted by lithium-ion batteries (LIBs) and compressed hydrogen storage (CHS) is evaluated. The work presented in [22] grounds on the harmonization of LIBs LCA analyses provided by [23], but it is possible to find in literature other case studies where this methodology is applied to alternative types of batteries [24–28], power to gas hydrogen production [29] and capacitors [30]. Connected to the LCA analysis is the exergo-environmental analysis (EEnvA), which is an advanced environmental impact assessment tool. The EEnvA enables to evaluate how the loss of energy quality affects the environmental impacts, through the weighting of exergy, and it is especially useful when applied to solar thermal systems [31].

Therefore, in the present study, alongside an exergo-economic analysis, an exergo-environmental analysis of a solar integrated thermo-electric energy storage system is carried out. The analysis has been performed for a selected reference study of a specific site (Crotone, southern Italy). The coupling of exergo-economic and exergo-environmental analyses allow drawing more in-depth considerations on the management of the system, enabling to evaluate the correct seasoning functioning of the TEES systems, not only from an economic point of view, as highlighted in [32], but also from an environmental impact perspective. Economic analysis has been here enriched by a sensitivity analysis, while the discussion on environmental aspects appears for the first time.

In Section 2, the system design and the methodology applied to evaluate TEES economic and environmental impact is carefully described. Section 3 contains the discussion and interpretation of the results. Finally, Section 4 contains the conclusions of the study.

2. TEES Description and Methods of Analysis

2.1. Description of Thermo-Electric Energy Storage System

The proposed TEES configuration has been introduced in a previous work [32], which dealt with the exergo-economic analysis of the proposed system. The storage system uses sensible heat liquid reservoirs, both for the cold and hot storage. The reason for this choice arose by the need for easy and fast control of the mass flow rate, aimed at correctly coupling the heat capacities in the heat exchangers both in the charging and discharging times. The proposed solar integrated TEES consists of three main sections: a trans-critical CO_2 power cycle (PC), a supercritical CO_2 heat pump (HP) and a subcritical R134a refrigeration cycle (RC). The inverse cycles (HP and RC) recharge the storage reservoirs (hot water cold reservoir, HWCR and hot water hot reservoir, HWHR and cold medium cold reservoir, CMCR and cold medium hot reservoir, CMHR) and make use of the solar energy during the daylight, both through thermal and electric energy conversion. A large fraction of the PV output is directed to satisfying the consumer's electric loads (the system is thought in support of a local micro or mini-grid), but, as frequently happens in good climates, there is at noon a surplus production of PV electricity, which is directed to store heat in the HWHR (through the HP) and cold in the CMCR (through the RC). The main power cycle PC works between the two average temperature levels of the HW and CM reservoirs during the discharging time, producing the power output. At present, the model just operates the PC at full power without any modulation (which would imply an off-design model of the PC). The efficiency of the system is enhanced by introducing a pre-heating of the main cycle working fluid through the utilization of an intermediate temperature reservoir (intermediate hot reservoir—IHR and intermediate cold reservoir—ICR), which is heated directly through solar thermal energy.

Figures 1 and 2 show the schematic of the heat pump and power cycles. A supercritical CO_2 cycle is proposed for the heat pump, because of the opportunity to recharge the hot reservoir at a relatively high temperature (145 °C). The heat pump configuration includes an expander, which replaces the commonly used throttling valve, aimed at improving the coefficient of performance (COP) [33]. The compressor is powered by the excess electricity available in the daytime from the photovoltaic (PV) solar field, while the evaporator temperature is kept at an intermediate level (95/40 °C) through the utilization of thermal solar collectors, which are connected by a three-way valve to an IHR. It is also utilized for the pre-heating of the power cycle working fluid.
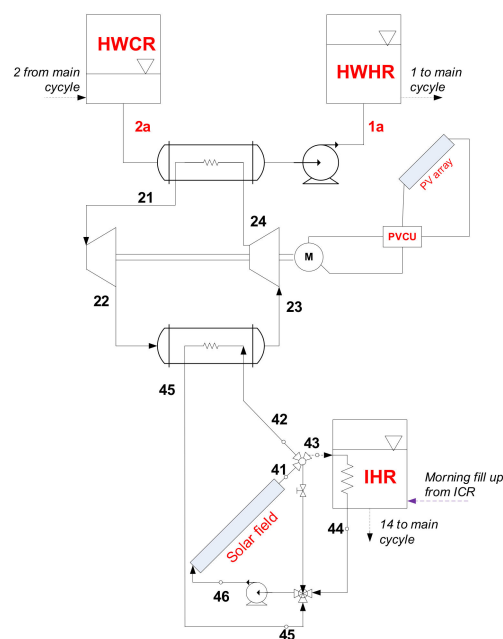

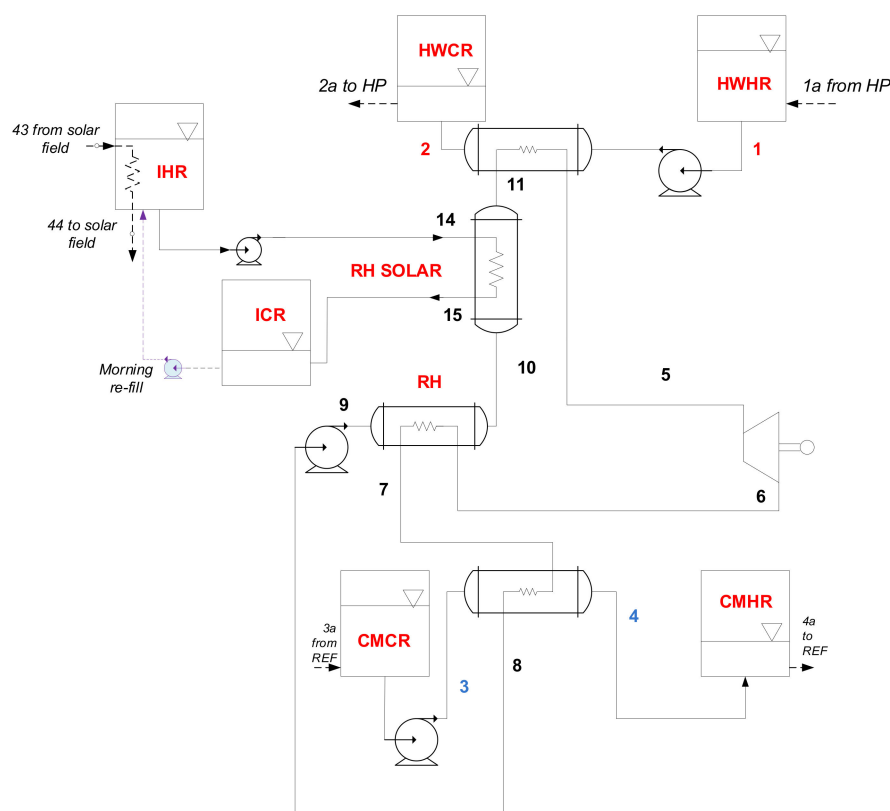**Figure 1.** Scheme of the solar-assisted heat pump cycle.

Figure 2. Scheme of the power cycle.

The proposed power cycle implements a trans-critical CO_2 configuration, which is a favorable solution considered the temperature range of both the hot and cold sinks (HW and CM reservoirs). The IHR allows the time de-coupling from the availability of the solar resource during the discharging time, which usually does not take place during the daytime.

The considered refrigeration cycle is a standard configuration arrangement using R134a as working fluid (which is suitable considering the limited cold conditions in the CM reservoirs, −10 to −20 °C). The objective of this inverse cycle is recharging the cold storage reservoirs (which are filled with water mixtures with appropriate anti-freeze additives, such as NaCl, $CaCl_2$ or Ethylene Glycol). The utilization of cold storage reservoirs allows increasing the pressure ratio of the turbine and, therefore, the increase of power output and efficiency of the cycle. The presence of low-temperature cold storage is of paramount importance if suitable roundtrip efficiency is coveted. The working parameters of the whole system can be found in [32].

The sizing of the solar fields refers to the specific location (Crotone, southern Italy), utilizing a single-reference-day (in May, for instance) quasi-dynamic model approach. It was agreed that analysis of system behavior during a single hour on a given day cannot represent the design point simulation of the system. By relying on an energy source of intermittent nature, authors have decided to use the term of a representative day instead. It became then a reference case for design day analysis. A single-reference-day of the month is created by using the source meteorological data from the Meteonorm database. The relevant data (direct, diffuse solar radiation and ambient temperature) are extracted every 60 min over one year. These data are processed to generate 12 average days statistically representative for each month of the year. The radiation and ambient temperature profiles were imported as Lookup Tables inside the dynamic simulation code, which was programmed using Engineering Equation Solver (EES). The quasi-dynamic approach rests on performing a simulation using a marching-forward procedure if meteorological data are considered, neglecting however more complex inertia phenomena during design analysis.

Commercially available flat plate solar collectors were assumed for the solar thermal field (η_0 = 0.719, a_1 = 1.45 W/(m^{2}K), a_2 = 0.0051W/(m^{2}K^2)). The number of solar collectors was determined by the heat demand from the heat pump evaporator, and the required temperature of the IHR reservoir; while the number of PV panels was obtained knowing the required power by the compressors of the inverse cycles. Commercially available polycrystalline modules were considered [34].

An off-design approach was then applied to assess the behavior of the whole system throughout the year and its dependence on the outer conditions. For off-design simulation, it is assumed that the size of all components within the system are already known, as specified in [32], and their performance can only be affected by independent external energy inputs or by involving some control procedure. The off-design analysis was solved numerically in EES through a time-forward simulation, assuming a length-adaptive time step, defined as the required time for the volume of heat transfer fluid (HTF) to close the loop in the solar field. The off-design analysis allows for the investigation of the capability of the charging cycles to load the reservoirs under the assumptions of variable meteorological conditions. Variable meteorological conditions are affecting solar thermal collectors and PV array output. Moreover, changing load conditions are also reflected by a performance curve applied to the turbine model. Table 2 summarizes the main design parameters of the thermo-electric storage system, which are fully described in [32].

Table 2. TEES design operating parameters.

Variable	Value
Power cycle	
T_1, T_2 (HWR)	95/145 °C
p_{HWR}, p_{IHR}, p_{CMR}	1800/100/100 kPa
$\dot{m}_{HW}$	1 kg/s
T_{14}, T_{15} (RH SOLAR)	95/40 °C
p_5	12,000 kPa
$\Delta T_{HOT} = T_1 - T_5 = \Delta T_{SOLAR} = T_{14} - T_{11}$	5 °C
$\Delta T_{COLD} = T_8 - T_3$	10 °C
T_3, T_4 (CWR)	−20/−10 °C
ε_{RH}	0.8
η_t, η_p	0.9/0.8
Operation Time (Power Cycle)	h
Heat Pump Cycle	
$\Delta T_{CO2-HW} = T_{21} - T_{2a}$	5 °C
$p_{min,HP}$	13,500 kPa
$\Delta T_{solar-CO2} = T_{42} - T_{23}$	5 °C
Refrigeration Cycle	
$\Delta T_{COLD} = T_{31} - T_0$	10 °C
$\Delta T_{EVA} = T_{3a} - T_{32}$	5 °C
Solar thermal collector fields	
Location	Crotone, Italy
Month for reference day	May
The slope of solar collector	45° towards South
η_0	0.719
a_1	1.45 W/(m^{2}K)
a_2	0.0051 W/(m^{2}K^2)
A_{sc}	1.6 m^2
$T_{41} = T_{42} = T_{43}$	95 °C
$\Delta T_{HTF} = T_{42} - T_{45} = T_{43} - T_{44}$	10 K
Collectors arrangement	Parallel in 10 rows

2.2. Exergo-Economic Models

It is assumed that to rationally assess the cost-effectiveness of a given plant, the economic costs should be rather assigned to exergy than to energy. This approach can be accepted if one remembers that exergy is seen as the indeed useful part of energy. The exergo-economic analysis combines the exergy analysis and the economic models, to provide the user with a clear and efficient evaluation of the cost-effectiveness of each component of the power plant, introducing the costs per exergy unit [35]. The exergy analysis is useful to assess not only the efficiency of energy systems but also the irreversibilities of each component [36]. It is done by application of the First and Second laws of thermodynamics. In the present work, the exergy is calculated at each point (j-th stream) of the system by simply applying its definition, which is the maximum work achievable from the interaction between the analyzed process and the environment (1):

$$\dot{Ex}_j = \dot{m}_j\left[\left(h_j - h_o\right) - T_o\left(s_j - s_o\right)\right] \tag{1}$$

Knowing the exergy rate assigned to each stream, an exergy balance is provided for each component remembering about exergy destruction and loss occurring within.

The developed economic model determines the daily costs of each component. The annual investment cost is calculated from (2):

$$Z_k^{an} = \frac{IR\cdot(1 + IR)^n}{(1 + IR)^n - 1}\,\dot{Z}_k \tag{2}$$

where:

- IR is the interest rate, which was assumed at 8%.
- n is the year lifetime, here assumed at 20 years.
- $\dot{Z}_k$ is the sum of cost rates associated with investments for the k-th component.

While estimating the purchase costs of each component of the systems, the authors decided to take advantage of findings presented by Henchoz et al. in [31] and compared them with cost functions given in the thermo-economic literature [37]. Since a storage-power cycle of similar principle was investigated in [31], with results consistent with those present in literature, it is expected that the applied cost functions are reliable. The cost functions applicable to the system components are presented in Table 3. Costs were updated to 2018 values, by using the CEPCI (Chemical Engineering Plant Cost Index) indexes [38] and by applying a proper €/\$ currency exchange rate. Solar collectors cost was assumed as a function of the surface area, at 210 \$/m^2 [39]. The PV modules' investment cost was assumed at 250 \$/module [40]. The applied currency exchange rate was 0.877 €/\$.

Table 3. Cost functions for the equipment [29,34].

Component	Function [10^3 \$, 2009]
Turbine	$1.5\cdot \dot{W}_T{}^{0.6} + 10$
Compressor	$6\cdot \dot{W}_C{}^{0.6} + 10$
Pump	$44\cdot \dot{V}_{wf}{}^{0.75} + 20$
Heat Exchanger	$0.3\cdot A_{HE}{}^{0.82} + 1$
Reservoir (HWHR/HWCR, CMHR/CMCR, IHR/ICR)	$0.2\cdot V_k{}^{0.785} + 2$

The exergo-economic approach outlined in [35,36] was then adopted by defining, for each component k, a cost balance equation, as shown in (3).

$$\dot{C}_{P,k} = \dot{C}_{F,k} + \dot{Z}_k$$
$$c_{P,k}\dot{Ex}_{P,k} = c_{F,k}\dot{Ex}_{F,k} + \dot{Z}_k \tag{3}$$

where:

- $\dot{C}_{P,k}$ and $\dot{C}_{F,k}$ are the cost rates associated respectively with exergy products and fuels.
- $c_{P,k}$ and $c_{F,k}$ are the costs per unit of exergy of product or fuel

Coupled to the cost balances, auxiliary equations were required to solve the system of equations, therefore the model suggested in [35,41] was applied. The solar radiation was assumed as costless.

The exergy destruction cost rate was calculated through (4):

$$\dot{C}_{D,k} = c_{F,k} \cdot \dot{Ex}_{D,k} \tag{4}$$

Finally, an exergo-economic factor, which associates the investment cost of the component to the sum of the investment cost and the cost of exergy destruction, was calculated through (5):

$$f_k = \frac{\dot{Z}_k}{\dot{Z}_k + \dot{C}_{D,k}} \tag{5}$$

All calculations were integrated over the day, considering the average reference day of each month. The yearly investment cost of the overall system also includes installation and maintenance costs, which were assumed at 20% of the total investment cost of the system [35].

The exergo-economic analysis was supplemented by a sensitivity analysis. It was performed in order to assess the susceptibility of levelized cost of electricity to change. The independent variable is the length of operational season.

2.3. LCA Model

LCA is one of the most widespread methods for the evaluation of the environmental impact and, according to the ISO 14040 and ISO 14044 regulations [42] it's defined as a four steps methodology including goal and scope definition; life cycle inventory (LCI); life cycle impact assessment (LCIA) and life cycle interpretation.

In the context of this article, the goal of the LCA is the estimation of the environmental impacts of a TEES system. An open-source software, named openLCA [43] and the database Ecoinvent 3.4 [44] was used for the environmental assessment of PV assisted TEES during daily charge and discharge cycles. The TEES eco-profile was compared to LIBs and CHS working in the same conditions. Furthermore, a pumped hydro storage system was considered. The functional unit of the LCA was set to 1 MWh of output electricity. Concerning the definition of the system boundaries, a 1% cut-off was set, excluding all those flows whose contribution to the overall emissions, raw materials and energy consumption is lower than that percentage. This allows fast calculations and can be done with a simple command in openLCA that was enabled for all the analyzed systems (TEES, PHS, LIBs, CHS) to guarantee the same cut-off conditions. Furthermore, coherently with the exergo-economic analysis, the TEES piping was not considered in the analysis and, consequently, also the amount of fluid inside it. On the other hand, the amounts of water and antifreeze liquid (calcium chloride) were evaluated based on the CWR and HWR volumes and temperatures.

As no primary data are available, Ecoinvent represents a reliable source of information. Thanks to the processes contained in the database, the materials depletion and all the emissions to the environment were estimated considering the construction, operation and maintenance, and disposal phases. The inventory data are collected in Table 4; although the system is supposed to be installed in

Crotone, none of the Ecoinvent processes used in the LCI has Italy as a geographical reference, therefore Switzerland (CH) has been used as a proxy. To estimate how the choice of the reference location affects the results, global (GLO) processes valid for every location will be also considered.

Considering the size of the solar plant, the land occupation represents a non-negligible part of the inventory and it has been modeled assuming that the system is installed in an industrial area.

Table 4. Life Cycle Inventory of the TEES system.

Flow	Amount	Unit	Process
Pump PC	696	Items	pump production, 40 W—CH
Turbine PC	1.73	Items	micro gas turbine production, 100 kW electrical—CH
Compressor HP	7.85	Items	air compressor production, screw-type compressor, 4 kW—RER (Europe)
Turbine HP	1.22	Items	air compressor production, screw-type compressor, 4 kW—RER
Throttle Valve RC	500	g	average for metal product manufacturing—RER
Compressor RC	3.55	Items	air compressor production, screw-type compressor, 4 kW—RER
Sol. collectors	320	m^2	evacuated tube collector production—GB
	6400	m^2·yr	Occupation, industrial area
IHR tank	4.59	Items	heat storage production, 2000 L—CH
HWR reservoir	3.74	Items	heat storage production, 2000 L—CH
CMR reservoir	0.05	Items	water storage construction—CH
PV panels	291.2	m^2	photovoltaic panel production, multi-Si—RER
	5824	m^2·yr	Occupation, industrial area
Plane HE	20	m^2	market for tin plated chromium steel sheet, 2 mm—GLO stone wool production—CH
Shell and tube HE	197	m^2	market for chromium steel pipe—GLO average for chromium steel product manufacturing—RER stone wool production—CH
Water	55,284	kg	market for water, deionised, from tap water—Europe without Switzerland
Calcium Chloride	32,750	kg	market for calcium chloride—GLO
Maintenance	3	Items	heat and power co-generation unit, 160 kW electrical | maintenance—RER market for maintenance, refrigeration machine—GLO

The electricity output over the TEES lifespan *T* (20 years) depends on its actual operation time. Five possible scenarios were proposed because, depending on the solar radiation, maintaining the plant operative might not be, in principle, economically convenient.

Some further information about LIBs is necessary to perform the analysis: the battery energy density, the efficiency, and the lifespan are respectively set to 116.1 Wh/kg, 90% and 1000 cycles [17,45]. Concerning the CHS, the storage system is composed of solid oxide fuel cells, solid oxide electrolyzers and a storage tank for the compressed gas accumulation. The inventory of Type III (350 bar) and Type IV (700 bar) hydrogen tanks and their expected lifespan (10 yrs) is provided by literature [46]. The fuel cells' environmental performances were modeled thanks to an Ecoinvent process, that can be also used as a proxy for the electrolyzer. Literature provides values for CHS roundtrip efficiency (67%) [47] and fuel cells lifespan, set to 48,000 h [44].

The LCI of the systems which, in this study, are compared to the TEES is described in Table 5.

Both the LIBs and CHS storage systems are designed to be charged by the PV system during the day and discharged during the night, similarly to the TEES. For this reason, they are supposed to perform one full cycle per day for a period of *T* (20 yrs). Another consequence is that the design value of stored energy is set to the maximum daily PV productivity *E* (394 Wh). Based on these assumptions, the amount of necessary batteries is:

$$m = \frac{E}{DoD \cdot d} \cdot \frac{T \cdot 365}{N} \tag{6}$$

where *DoD*, *d*, and *N* are respectively the depth of discharge (%), the energy density (Wh/kg) and the lifespan (cycles).

Table 5. Life Cycle Inventory of the PHS, LIBs and CHS.

Flow	Amount	Unit	Process
PHS			
Electricity	1	MWh	electricity production, hydro, pumped storage—IT
LIBs			
Inputs			
PV panels	291.2	m^2	photovoltaic panel production, multi-Si—RER
	5824	m^2·yr	Occupation, industrial area
Inverter	2	Items	inverter production, 500 kW—RER
Battery charger	56.5	kg	charger production, for electric scooter—GLO
Batteries	30,967	kg	battery production, Li-ion, rechargeable, prismatic—GLO
Outputs			
Electricity	1862	MWh	Reference Flow
CHS			
Inputs			
PV panels	291.2	m^2	photovoltaic panel production, multi-Si—RER
	5824	m^2·yr	Occupation, industrial area
Electrolyser	0.4	Items	fuel cell production, solid oxide, 125 kW electrical—CH
Fuel Cell	1.83	Items	fuel cell production, solid oxide, 125 kW electrical—CH
Inverter	2	Items	inverter production, 500 kW—RER
Storage Tank	98.5	Items	Type II and Type IV Tank production, adapted from [26]
Outputs			
Electricity	1058.9	MWh	In case of pressurization up to 350 bar
	1011.4	MWh	In case of pressurization up to 700 bar

Concerning the CHS storage, a 172 kW solid oxide fuel cell and a 37 kW electrolyzer have been chosen because their power is respectively equal to the turbine and the PV plant of TEES. The mass of Type III and Type IV storage tanks is obtained scaling an 8 kWh tank whose LCI is analyzed by [46]. The output electricity must be evaluated considering the roundtrip efficiency of the storage system, the efficiency of common inverters (set to 90%) and charge controllers (set to 98%) and of the electric connections (set to 90%). In the case of CHS, the energy used to compress the gas must also be subtracted [47].

In the LCIA, some calculation methods convert the LCI to environmental impacts, classifying them in categories. The classification and characterization don't allow the calculation of a single score impact value, which can be obtained thanks to a normalization and weighting set. This is very important, as it allows comparing easily two different systems and to perform the related exergo-environmental analysis. The main drawback of a single score impact calculation is that normalization and weighting operations add uncertainty to the LCA model. For such reason, results should always be discussed also at the midpoint level, which means using a problem-oriented approach to analyze the environmental issues of the product system without evaluating their effects. Seventeen midpoint environmental impact categories are proposed by ReCiPe (version 2016) but some of them are largely more consolidated than others. For instance, global warming potential (GWP) represents the most widely analyzed category, but also acidification potential (AP), human toxicity potential (HTP), particulate matter formation (PMF) and photochemical ozone formation (POF) are usually considered as the most relevant for energy storage studies [17]. Furthermore, the evaluation of single score results summarizing all the impact categories was carried out thanks to a European normalization and weighting set (ReCiPe Europe H/A), as the selected location is Crotone. The unit of measurement commonly used for single score environmental impact is the eco-point, abbreviated as Pts, introduced by Eco-indicator 99 and then adopted by other LCIA methods like ReCiPe [48].

2.4. Exergo-Environmental Model

An integral exergo-environmental analysis was carried out over the representative day of each month of the year, coherently with the thermo-economic analysis [49]. The environmental cost rates related to each j-stream $\dot{B}_j$ (Pts/s) were allocated to their exergy content $\dot{Ex}_j$ (kWh/s) to evaluate the specific environmental impacts b_j (Pts/kWh) through (7):

$$b_j = \frac{\dot{B}_j}{\dot{Ex}_j} \tag{7}$$

This methodology is based on the solution of impact balances performed for every *k*-component, using (8):

$$\sum \dot{B}_{j,k,in} + \dot{Y}_k = \sum \dot{B}_{j,k,out} \tag{8}$$

where $\dot{Y}_k$ (Pts/s) is the environmental impact rate associated with the construction, operation and maintenance, and disposal phases. This parameter is connected with the LCA results, expressed considering 1 MWh as a functional unit (Pts/MWh). So, the single score impact was multiplied by the yearly productivity; after that, an impact rate $\dot{Y}_k$ was achieved by the ratio with the charge and discharge time.

The environmental costs per unit of exergy (Pts/kWh) of product $b_{P,k}$ and fuel $b_{F,k}$ were defined according to the exergo-economics. This allowed the evaluation of an environmental cost rate $\dot{B}_{D,k}$ (mPts/s) associated with the exergy destructions occurring inside each component through (9):

$$\dot{B}_{D,k} = b_{F,k} \cdot \dot{Ex}_{D,k} \tag{9}$$

Based on these definitions, an exergo-environmental factor $f_{d,k}$ representing the percentage contribution of $\dot{Y}_k$ compared to the total $\dot{B}_{D,k} + \dot{Y}_k$, was calculated using (10):

$$f_{d,k} = \frac{\dot{Y}_k}{\dot{B}_{D,k} + \dot{Y}_k} \tag{10}$$

3. Results

As mentioned above, detailed energy, exergy and exergo-economic analysis results of the seasonal simulation have already been published by the authors in [32]. The seasonal off-design simulation was performed using as input fixed geometry of the system found for design day analysis (May in Crotone). The main important design sizes are the volumes of the tanks (V_{HWR} = 3.74 m^3, V_{IHR} = 9.175 m^3. V_{CMR} = 65.5 m^3), the number of solar collectors installed (200), number of PV modules installed (224). For the design day simulation, during which the charging lasted 7 h and the discharge time was 1 h, it was possible to generate 172,6 kW in the turbine. The marginal round-trip efficiency was then 51%. If the simulation was repeated in the off-design mode for reference days of other months (April–September), the input simulation data included meteorological conditions, size of solar fields, maximum volumes of reservoirs. Variable outer conditions affected i.a. the duration of charging, discharging, power output, round-trip marginal efficiency. Quantitative results of off-design analysis are available in [32].

The analysis in here presented research was firstly extended by an exergo-economic sensitivity analysis with operational season length being the sensitivity factor. The system performance was then assessed in terms of LCA and exergo-environmental analysis. To maintain the originality of the research and to avoid duplication of results presentation, only the new findings are here cited.

3.1. Exergo-Economics

Table 6 introduces a summary of the exergo-economic sensitivity analysis results. The sensitivity analysis indicates how the change of operation periods (from summer months only to the whole year) would affect the levelized cost of the produced electricity. It is clear, as expected, that the yearly working period significantly affects LCOE. Anyhow, it is interesting to notice how the decrease of LCOE with the yearly working period is not linear and the gradient is more relevant in the short periods: for example, being able to extend the exploitation of the TEES from 3 to 5 months per year in spring-summer months reduces the LCOE of about 40%. On the other hand, further extensions of TEES yearly operational time towards seasons with less insulation leads to a progressive marginalization of LCOE reduction.

Table 6. Annual operational details for TEES systems operated in Crotone (39.08 °N, 17.11 °E), considering different possible working periods.

	June–August	May–September	April–October	January–December
Total operation time of TEES (h/year)	734	1234	1744	2800
Productivity (MWh/year)	15.1	24.9	34.1	49.0
Annual average LCOE (€/kWh)	2.76	1.67	1.22	0.85

Levelized cost of electricity is treated as a break-even economic indicator, showing the minimum sale price at which the plant generates enough revenue during lifetime (here 20 years with assumed discount rate) to pay back all of the associated costs. If a simple payback period were calculated and no discounted cash flows were analyzed, it would happen already after 10 years.

3.2. LCA

The midpoint results of LCA are presented in Figure 3. Considering the GWP (Figure 3a) and AP (Figure 3b) impact categories, TEES is assessed as the second less impactful storage system after LIBs, mainly because of the carbon dioxide and the sulfur dioxide emissions dealing with the industrial heat required by the production of the components. Particularly, considering the GWP category the PV plant (24.1%), the CMR (16.5%) and the solar thermal system (13.9%) are the most impactful components. Similarly, the thermal solar system (25.9%), the CMR (16.7%) and the PV plant (15.1%), represent the main contributors to the TEES burden for the AP category too. The results calculated for HTP (Figure 3c) are slightly different as TEES is assessed as more impactful than PHS but less than LIBs, whose copper content (mainly present in the current collector) affects its environmental performances for this category. Solar collectors are largely the most impactful TEES components for AP because of the big amount of copper used in the absorber. Concerning the PMF category, TEES is assessed as a less sustainable solution than both PHS and LIBs (Figure 3d): PM_{10} and $PM_{2.5}$ are mainly produced during the industrial manufacturing of solar thermal (20.7%) and PV (16.3%) panels. The results obtained for the POF impact category (Figure 3d) are similar to those of GWP and HTP because TEES is the second most sustainable system after LIBs. In this case, the nitrogen oxides emitted during the manufacturing of the thermal solar plant (20.8%), the PV plant (16.3%) and the HEs (14.1%) are the main responsible for the impact. For every impact category, it is possible to appreciate that both CHS solutions represent the most impactful storage system and the storage tanks represent the major contributor to this impact (from 40% to 56%, depending on the category). Figure 3 also shows that, depending on the operation time of the system, the TEES could become more impactful than the competitors for all the impact categories.
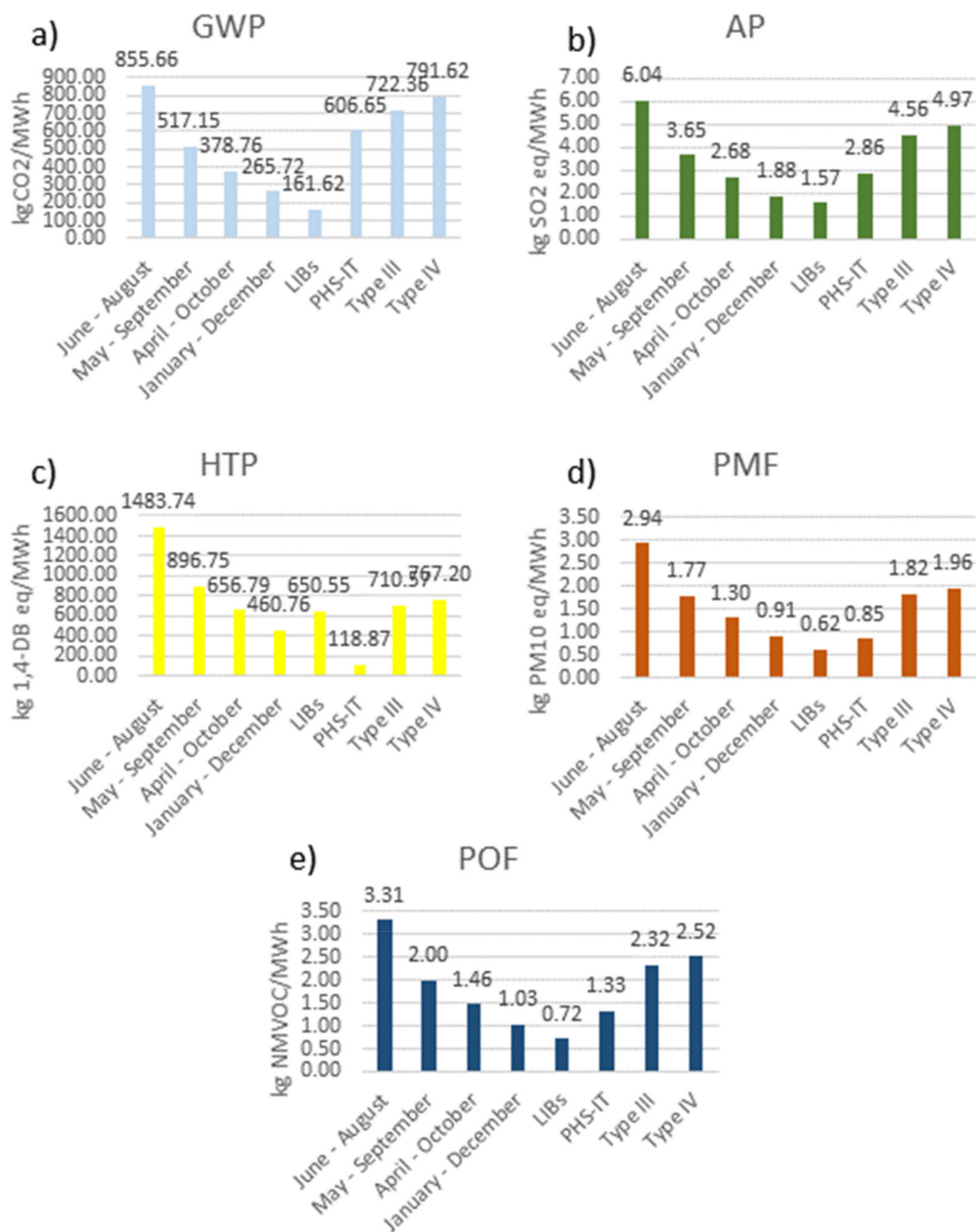
Figure 3. Midpoint environmental impacts of the analyzed systems for the impact categories: (**a**) GWP; (**b**) AP; (**c**) HTP; (**d**) PMF and (**e**) POF.

The single score environmental impacts of the TEES are shown in Figure 4, where they are represented per unit of output electricity, coherently with the choice of the functional unit. The environmental performances of TEES have been assessed varying the operation time whereas the other storage systems are supposed to be always operative. This affects the resulting eco-profiles because, coherently with the functional unit definition, the environmental impacts are divided by the productivity of the solar integrated TEES. Therefore, enlarging the operation time guarantees an environmental benefit as an effect of higher energy output. As TEES is powered by PV, this benefit is higher whether it works in months of high solar. For instance, in case the system is operative only in the summer months (June–August), the environmental impact is 202.84 Pts/MWh but if May and September, when radiation is powerful, are also considered the impact falls to 122.59 Pts/MWh. Extending the working time, the environmental advantage is progressively reduced because the system

works in low radiation periods. Indeed, the burden decreases to 89.79 Pts/MWh when including April and October and to 62.99 Pts/MWh in case the full-year operation. Changing geographical reference to the processes in Tables 3 and 5 the results are slightly different as TEES environmental impact is about 5% higher.
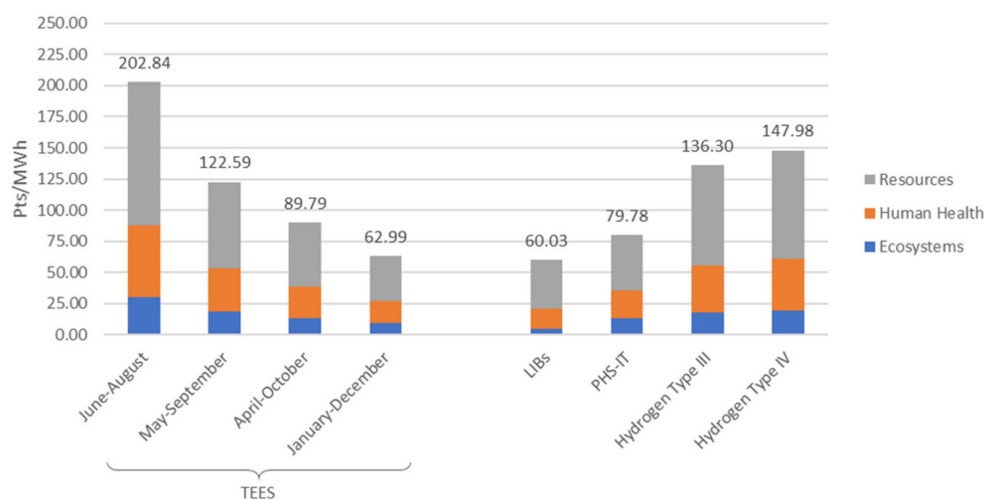

Figure 4. Single score environmental impacts of the analyzed systems.

The assessment of the TEES single components contribution represents an input for the exergo-environmental analysis: both the thermal solar and PV give the highest contribution to the single score impact, at 21% level. They are followed by the concrete CMR (18%), whose high volume determines a relevant burden connected with the consumption of raw materials and calcium chloride, used as antifreeze.

The single score impacts illustrated in Figure 4 are obtained weighting all the 17 midpoint categories proposed by ReCiPe. These indicators contribute to the total impact in different measures: particularly, GWP represents 14% of the single score and affects both human health and ecosystems damage categories; the depletion of fossil and metal resources contributes together to about 60% of the single score as underlined by the size of the grey column in Figure 4. The other indicators have minor relevance in the TEES eco-profile.

Another impactful component is the turbine in the TEES PC, whose burden represents 12% of the total. Concerning the comparison with other storage systems, a $LiMn_2O_4$ LIB bank was designed to store the PV output energy in the average day of the most productive month (394 kWh). Its environmental impact (60.03 Pts/MWh) is comparable with the TEES: even though these batteries are more efficient (90% roundtrip efficiency [17]), their lifespan is much shorter than TEES. Indeed, assuming a discharge time of 1 h (similarly to TEES) and an 80% depth of discharge, this type of batteries can perform 1000 cycles [38], responding to about three years. Batteries are often installed for household applications, whereas pumped hydro storage represents the most diffused high-power competitor to produce and store dispatchable energy on a large scale. The environmental impact of a representative PHS system installed in Italy was evaluated using an Ecoinvent process [44] per MWh of output electricity and its single score damage results to be higher than that of TEES (+27%) and LIBs (+33%). Concerning the hydrogen storage systems, two scenarios differing for the operative pressure, and consequently for the type of storage tank (type III and type IV), were proposed. In both cases, their environmental impact is much higher than that of the other competitors (about two times higher than TEES) because of the low roundtrip efficiency (61%) and the use of rare construction materials in electrolyzers and fuel cells manufacturing (platinate materials). The above results are evaluated using a classic LCA but a novel approach named prospective LCA also exists and may bring to different findings. This methodology is commonly used to compare systems having different

maturity levels: the future characteristics of emerging technologies can be forecasted to valorize their future potential [50].

3.3. Exergo-Environmental Analysis

The results of the exergo-environmental analysis are collected in Table 7, using a reference day of May to visualize the results collecting the following parameters:

- $\dot{Y}_k$ is the life cycle environmental impact of the TEES components, that is calculated from the LCA: first a contribution analysis is done to evaluate the burden of every TEES component as Pts/MWh; then this result is converted to Pts/day multiplying it by the solar TEES productivity in the reference day.
- $\dot{B}_{D,k}$ is the environmental impact of the exergy destructions that estimates the environmental drawback of losing energy quality due to thermodynamic irreversibility.
- $\dot{Y}_k + \dot{B}_{D,k}$ is the total environmental impact considering the above contributions.
- $b_{F,k}$ is the specific environmental impact of the inlet exergy flows to the components.
- $b_{P,k}$ is the specific environmental impact of the output exergy flows from the components.
- $f_{b,k}$ represents the percentage contribution of $\dot{Y}_k$ to the total environmental impact.

Concerning the total environmental impact ($\dot{Y}_k + \dot{B}_{D,k}$), which includes both the burdens related to the components life cycle and the exergy destructions, the CMR resulted as the most impactful component, representing the 20% of the total score. 29% of the CMR impact value is related to the specific cost of the component ($\dot{Y}_k$), whereas 71% is attributable to the exergy destructions ($\dot{B}_{D,k}$). Indeed, the thermodynamic irreversibility occurring inside the CMR contributes to 22% of the total impact of exergy destructions.

Table 7. Results of the exergo-environmental analysis on a reference day of May.

k	Component	$\dot{Y}_k$ (Pts/day)		$\dot{B}_{D,k}$ (Pts/day)		$\dot{Y}_k + \dot{B}_{D,k}$ (Pts/day)		$b_{F,k}$ (Pts/kWh)	$b_{P,k}$ (Pts/kWh)	$f_{b,k}$ (%)
1	Condenser PC	0.09	1%	0.74	3%	0.83	2%	0.05	0.06	11%
2	Pump PC	0.45	4%	0.51	2%	0.96	3%	0.09	0.13	47%
3	RH—int PC	0.17	1%	0.15	1%	0.32	1%	0.07	0.28	52%
4	RH—solar PC	0.50	4%	0.88	4%	1.37	4%	0.03	0.06	36%
5	HTHE PC	0.28	2%	0.13	1%	0.42	1%	0.04	0.05	68%
6	Turbine PC	1.34	12%	1.85	8%	3.19	9%	0.07	0.09	42%
7	Evaporator HP	0.02	0%	0.09	0%	0.11	0%	0.02	0.02	17%
8	Compressor HP	0.38	3%	0.39	2%	0.77	2%	0.02	0.03	49%
9	Condenser HP	0.07	1%	3.00	13%	3.07	9%	0.03	0.03	2%
10	Turbine HP	0.06	1%	0.32	1%	0.38	1%	0.03	0.04	16%
11	Condenser RC	0.18	2%	1.26	6%	1.44	4%	0.09	0.20	12%
12	Throttle Valve RC	0.00	0%	0.54	2%	0.54	2%	0.02	0.02	0%
13	Evaporator RC	0.09	1%	3.78	17%	3.87	11%	0.02	0.03	2%
14	Compressor RC	0.17	2%	0.36	2%	0.53	2%	0.01	0.01	33%
15	Sol. collectors	2.44	21%	0.00	0%	2.44	7%	0.00	0.02	100%
17	IHR tank	0.40	4%	0.57	3%	0.97	3%	0.02	0.03	41%
21	HWR reservoir	0.33	3%	3.11	14%	3.43	10%	0.03	0.04	9%
22	CMR reservoir	2.05	18%	4.93	22%	6.97	20%	0.03	0.05	29%
23	PV panels	2.40	21%	0.00	0%	2.40	7%	0.00	0.01	100%

The solar thermal and PV systems were estimated as the most impactful components in LCA, but since they just use sustainable solar energy, the environmental cost of the exergetic fuel is assumed to be zero as well as the impact of exergy destructions. Consequently, the contribution of thermal solar plants to $\dot{Y}_k + \dot{B}_{D,k}$ is reduced to 7%. Although their limited contribution to the LCA results, other impactful components are the evaporator in the refrigeration cycle and the HWR, because of

their relevant exergy destructions. The low exergo-environmental factor ($f_{b,k}$) evaluated for some components, like reservoirs and heat exchangers, is due to a high contribution of thermodynamic irreversibility and exergy destructions to the total environmental impact. The same findings can be obtained for the representative day of all the other months as well (Figure 5). Figure 5 is useful to understand that, in each month, the impact of the exergy destructions is higher than that of the components' life cycle, and that the total environmental impact varies in a range between 14.0 and 24.5 Pts/day. Energy systems fueled by fossils are typically characterized by high-impact exergy destructions because of the specific environmental burden of the fuel [50]. Contrarily, in this case, the contribution of life cycle impacts (in blue) is lower but not negligible compared to the exergy destructions impacts (in orange). This can happen when technologies like solar collectors or photovoltaic modules are involved in the system because they don't contribute to $\dot{B}_{D,k}$ but only to $\dot{Y}_k$ [21,51,52] as the specific impact of their fuel (solar energy) is zero. This consideration is valid for the typical day of each month.
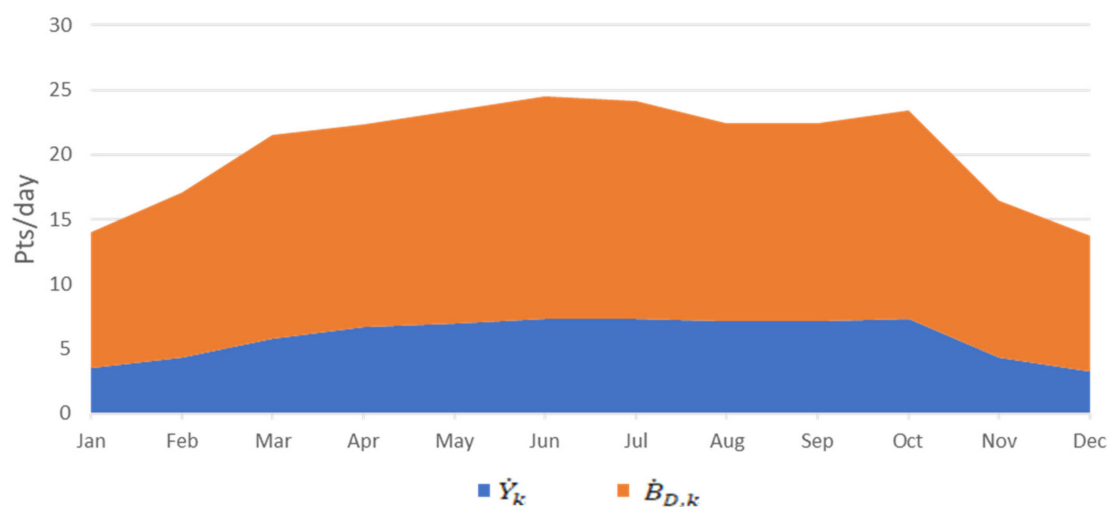

Figure 5. Total environmental impact of TEES as the sum of the burdens dealing with components and exergy destructions during the year.

4. Conclusions

The manuscript deals with the impact assessment of a solar TEES system by the means of exergo-economic and exergo-environmental analysis. The exergo-economic analysis does not reveal market-competitive results. The average annual levelized cost of electricity from the system is at least 2.5 times higher than currently binding electricity costs. However, it still might be considered attractive considering other standalone RES systems.

LCA results are first discussed at the midpoint level, to analyze the environmental problems of TEES for several categories (GWP, AP, HTP, PMF, and POF). These results show that in case of full working time, TEES eco-profile can be compared with LIBs and PHS, whereas CHS is the less sustainable energy storage system. If the yearly working time is reduced for economic reasons, TEES becomes less competitive from the environmental point of view. PV and solar thermal panels represent the main contribution to the impact for most of the selected categories. Furthermore, LCA provided the single score environmental impacts of the TEES components, which were inputs to the exergo-environmental procedure. These results do not substantially differ from midpoint results. Indeed, concerning both types of results visualization approaches, the Thermal Solar and PV panels give the highest contribution (21% of the single score), followed by concrete CMR (18% of the single score). The comparison with the environmental impact of competitive storage systems for dispatchable energy production like PHS and LIBs revealed single-score damage at the same level of TEES if the latter is operative in the range of half year. On the other hand, hydrogen storage systems, under two

possible different scenarios, showed a much higher environmental impact level over TEES (about two times higher). Referring to the total exergo-environmental impact of single components, CMR was the most critical (20% of the total score), mainly due to exergy destructions.

Finally, despite the highest contribution of solar thermal and PV to overall LCA impacts, their exergo-environmental score is reduced to 7%, following the assumption of zero environmental costs per unit of exergy of incoming solar radiation. As a concluding remark, the exergo-environmental analysis acts as an added value to the LCA results, because the environmental impact of some components, like heat exchangers or solar panels, are significantly different considering the effect of exergy destructions, as expressed by low exergo-environmental factors. For these reasons, the application of this methodology is recommended to better address the comparison of different energy storage systems.

This paper is very extensive and innovative because energy, exergy, exergoeconomic, and exergo-environmental analyses have been applied to TEES for the first time in the synergic approach. Nevertheless, some further work may be added in the future: TEES performances could be evaluated considering the productivity profile of a power plant, like a PV system, and a realistic load profile of a residential or industrial user. The system can dispatch energy to the grid depending on the economic convenience of time-variable tariffs and feed-in remuneration. These boundary conditions would affect affecting the size, the performances of the storage system, and consequently the results of the exergoeconomic and exergo-environmental analyses. Moreover the LCA approach adopted in this paper could be furtherly improved using prospective LCA.

Nomenclature

Symbols and acronyms

A	area, m^2
AP	Acidification Potential
$\dot{C}$	Cost rate associated with exergy transfer, €/day
$\dot{B}$	Impact rate associated with exergy transfer, €/day
CAES	Compressed air energy storage
CHS	Compressed hydrogen storage
CMR	Cold medium reservoir (common name for CMHR and CMCR assembly)
CMHR	Cold medium-hot reservoir
CMCR	Cold medium-cold reservoir
COP	Coefficient of performance
d	Energy density, Wh/kg
DoD	Depth of discharge, %
ES	Energy storage
Ex	Total exergy, kw
F	Exergo-economic factor, %
FS	Flywheel storage
GWP	Global Warming Potential
HP	Heat Pump
LIB	Lithium-Ion Battery
HWR	Hot water reservoir (common name for HWHR and HWCR assembly)

HWHR	Hot water hot reservoir
HWCR	Hot water cold reservoir
HTP	Human Toxicity Potential
ICR	Intermediate-heat cold reservoir
IHR	Intermediate-heat hot reservoir
IR	Interest rate
HTF	Heat transfer fluid
LAES	Liquid air energy storage
LCOE	Levelized cost of electricity (stored), €/kWh
m	Mass of the batteries, kg
N	Batteries lifespan, cycles
n	Operation year
PC	Power cycle
PHS	Pumped hydro storage
PMF	Particulate Matter Formation
POF	Photochemical Ozone Formation
PT	Eco-points
PV	Photovoltaic
PVCU	PV conversion unit
RC	Refrigeration cycle
RES	Renewable energy sources
RH	Reheater
S-TEES	Solar integrated thermoelectric energy storage
T	Reference time of the analysis, yrs
TEES	Thermoelectric energy storage
V	Volume, m^3
VRE	Variable renewables
$\dot{V}$	Volumetric flow rate, m^3/s
$\dot{W}$	Power, kw
Z	Cost rate associated with capital investment and O&M costs, €/day
Subscripts and superscripts	
C	Compressor
f	Fuel
he	Heat exchanger
k	Plant component
P	Product
p	Pump
t	Turbine
tank	Tank
wf	Working fluid (CO_2 in the main power cycle)

References

1. McPherson, M.; Tahseen, S. Deploying storage assets to facilitate variable renewable energy integration: The impacts of grid flexibility, renewable penetration, and market structure. *Energy* **2018**, *145*, 856–870. [CrossRef]
2. IRENA; OECD/IEA; REN21. *Renewable Energy Policies in a Time of Transition*. 2018. Available online: https://www.irena.org/-/media/Files/IRENA/Agency/Publication/2018/Apr/IRENA_IEA_REN21_Policies_2018.pdf (accessed on 2 July 2020).
3. ENEA Consulting. *Facts & Figures: Le Stockage d'Energie*; ENEA Consulting: Paris, France, 2012.
4. Ayachi, F.; Tauveron, N.; Tartière, T.; Colasson, S.; Nguyen, D. Thermo-Electric Energy Storage involving CO_2 transcritical cycles and ground heat storage. *Appl. Therm. Eng.* **2016**, *108*, 1418–1428. [CrossRef]
5. Morandin, M.; Mercangozz, M.; Hemrle, J.; Marechal, F.; Favrat, D. Thermoeconomic design optimization of a thermo-electric energy storage system based on transcritical CO_2 cycles. *Energy* **2013**, *58*, 571–587. [CrossRef]

6. Ren, J.; Ren, X. Sustainability ranking of energy storage technologies under uncertainties. *J. Clean. Prod.* **2018**, *170*, 1387–1398. [CrossRef]

7. Hadjipaschalis, I.; Poulikkas, A.; Efthimiou, V. Overview of current and future energy storage technology for electric power applications. *Renew. Sustain. Energy Rev.* **2009**, *13*, 1513–1522. [CrossRef]

8. Wang, J.; Lu, K.; Ma, L.; Wange, J.; Dooner, M.; Miao, S.; Li, J.; Wang, D. Overview of compressed air energy storage and technology development. *Energies* **2017**, *10*, 991. [CrossRef]

9. Abdi, H.; Mohammadi-ivatloo, B.; Javadi, S.; Khodaei, A.R.; Dehnavi, E. Energy Storage Systems. In *Distributed Generation Systems, Design, Operation and Grid Integration*; Butterworth-Heinemann: Oxford, UK, 2017.

10. International Energy Agency. Technology Roadmap Hydrogen and Fuel Cells [WWW Document]. 2015. Available online: http://ieahydrogen.org/pdfs/TechnologyRoadmapHydrogenandFuelCells-(1).aspx (accessed on 20 March 2020).

11. NREL. Energy Storage [WWW Document]. 2019. Available online: https://www.nrel.gov/docs/fy19osti/73520.pdf (accessed on 21 March 2020).

12. Luo, X.; Wange, J.; Dooner, M.; Clarke, J. Overview of current development in electrical energy storage technologies and the application potential in power system operation. *Appl. Energy* **2015**, *137*, 511–536. [CrossRef]

13. Tauveron, N.; Macchi, E.; Nguyen, D.; Tartière, T. Experimental study of supercritical CO_2 heat transfer in a Thermo-Electric Energy Storage based on Rankine and heat pump cycles. *Energy Procedia* **2017**, *129*, 939–946. [CrossRef]

14. Benato, A.; Stoppato, A. Pumped thermal electricity storage: A technology overview. *Therm. Sci. Eng. Prog.* **2018**, *6*, 301–315. [CrossRef]

15. Morandin, M.; Maréchal, F.; Mercangoz, M. Butcher, Conceptual design of a thermo-electrical energy storage system based on heat integration of thermodynamic cycles-Part A: Methodology and base case. *Energy* **2012**, *45*, 375–385. [CrossRef]

16. Morandin, M.; Maréchal, F.; Mercangoz, M. Butcher, Conceptual design of a thermo-electrical energy storage system based on heat integration of thermodynamic cycles-Part B: Alternative system configurations. *Energy* **2012**, *45*, 386–396. [CrossRef]

17. White, A.; Parks, G.; Markides, C.N. Thermodynamic analysis of pumped thermal electricity storage. *Appl. Therm. Eng.* **2013**, *53*, 291–298. [CrossRef]

18. McTigue, J.D.; White, A.J.; Markides, C.N. Parametric studies and optimization of pumped thermal electricity storage. *Appl. Energy* **2015**, *137*, 800–811. [CrossRef]

19. Liu, Y.; Wang, Y.; Huang, D. Supercritical CO_2 Brayton cycle: A state of the art review. *Energy* **2019**, *189*, 115900. [CrossRef]

20. Talluri, L.; Manfrida, G.; Fiaschi, D. Thermoelectric energy storage with geothermal heat integration–Exergy and exergo-economic analysis. *Energy Convers. Manag.* **2019**, *199*, 111883. [CrossRef]

21. Henchoz, S.; Buchter, F.; Favrat, D.; Morandin, M.; Mercangoz, M. Thermoeconomic analysis of a solar enhanced energy storage concept based on thermodynamic cycles. *Energy* **2012**, *45*, 358–365. [CrossRef]

22. Rossi, F.; Parisi, M.L.; Maranghi, S.; Basosi, R.; Sinicropi, A. Science of the Total Environment Environmental analysis of a nano-grid: A Life Cycle Assessment. *Sci. Total Environ.* **2020**, *700*, 134814. [CrossRef] [PubMed]

23. Peters, J.F.; Weil, M. Providing a common base for life cycle assessments of Li-Ion batteries. *J. Clean. Prod.* **2018**, *171*, 704–713. [CrossRef]

24. Weber, S.; Peters, J.F.; Baumann, M.; Weil, M. Life Cycle Assessment of a Vanadium Redox Flow Battery. *Environ. Sci. Technol.* **2018**, *52*, 10864–10873. [CrossRef]

25. Troy, S.; Schreiber, A.; Reppert, T.; Gehrke, H.G.; Finsterbusch, M.; Uhlenbruck, S.; Stenzel, P. Life Cycle Assessment and resource analysis of all-solid-state batteries. *Appl. Energy* **2016**, *169*, 757–767. [CrossRef]

26. Zackrisson, M.; Fransson, K.; Hildenbrand, J.; Lampic, G.; O'Dwyer, C. Life cycle assessment of lithium-air battery cells. *J. Clean. Prod.* **2016**, *135*, 299–311. [CrossRef]

27. Peters, J.; Buchholz, D.; Passerini, S.; Weil, M. Life cycle assessment of sodium-ion batteries. *Energy Environ. Sci.* **2016**, *9*, 1744–1751. [CrossRef]

28. Deng, Y.; Li, J.; Li, T.; Gao, X.; Yuan, C. Life cycle assessment of lithium-sulfur battery for electric vehicles. *J. Power Sources.* **2017**, *343*, 284–295. [CrossRef]

29. Parra, D.; Zhang, X.; Bauer, C.; Patel, M.K. An integrated techno-economic and life cycle environmental assessment of power-to-gas systems. *Appl. Energy* **2017**, *193*, 440–454. [CrossRef]

30. Smith, L.; Ibn-Mohammed, T.; Koh, S.C.L.; Reaney, I.M. Life cycle assessment and environmental profile evaluations of high volumetric efficiency capacitors. *Appl. Energy* **2018**, *220*, 496–513. [CrossRef]

31. Rossi, F.; Parisi, M.L.; Maranghi, S.; Manfrida, G.; Basosi, R.; Sinicropi, A. Environmental impact analysis applied to solar pasteurization systems. *J. Clean. Prod.* **2019**, *212*, 1368–1380. [CrossRef]

32. Fiaschi, D.; Manfrida, G.; Petela, K.; Talluri, L. Thermo-Electric Energy Storage with Solar Heat Integration: Exergy and Exergo-Economic Analysis. *Energies* **2019**, *12*, 648. [CrossRef]

33. Ferrara, G.; Ferrari, L.; Fiaschi, D.; Galoppi, G.; Karellas, S.; Secchi, R.; Tempesti, D. Energy Recovery By Means Of A Radial Piston Expander In A CO2 Refrigeration System. *Int. J. Refrig.* **2016**, *72*, 147–155. [CrossRef]

34. Schott Applied Power Corporation, High Efficiency Multi-Crystal Photovoltaic Module. Available online: http://abcsolar.com/pdf/schott165.pdf/ (accessed on 27 February 2019).

35. Bejan, A.; Tsatsaronis, G.; Moran, M. *Thermal Design and Optimization*; John Wiley & Sons, Inc.: New York, NY, USA, 1996.

36. Kotas, T.J. *The Exergy Method of Thermal Plant Analysis*; Butterworth-Heinemann: Oxford, UK, 1985.

37. Turton, R.; Bailie, R.; Whiting, W.; Shaeiwitz, J. *Analysis, Synthesis and Design of Chemical Processes*; Prentice Hall: Upper Saddle River, NJ, USA, 2003.

38. Chemical Engineering, Economic Indicators. Available online: https://www.chemengonline.com/site/plant-cost-index/ (accessed on 28 February 2019).

39. Kalogirou, S.A. *Solar Energy Engineering, Processes and Systems*, 2nd ed.; Academic Press: Cambridge, MA, USA, 2013.

40. Freecleansolar, 165W Module Schott SAPC-165 Poly. Available online: https://www.freecleansolar.com/165W-module-Schott-SAPC-165-poly-p/sapc-165.htm (accessed on 28 February 2018).

41. Lazzaretto, A.; Tsatsaronis, G. SPECO: A systematic and general methodology for calculating efficiencies and costs in thermal systems. *Energy* **2006**, *31*, 1257–1289. [CrossRef]

42. International Standards Organization. EN ISO 14040:2006-Valutazione del Ciclo di Vita. Principi e Quadro di riferimento. *Environ. Manag.* **2010**, 14040. Available online: http://www.eliosingegneria.it/i-nostri-servizi/tutela-dellambiente/75-valutazione-del-ciclo-di-vita-uni-en-iso-140402006 (accessed on 2 July 2020).

43. Greendelta. OpenLCA 2018. Available online: https://www.greendelta.com/ (accessed on 2 July 2020).

44. Moreno Ruiz, E.; Valsasina, L.; Fitzgerald, D.; Brunner, F.; Vadenbo, C.; Bauer, C.; Wernet, G. Documentation of changes implemented in the Eco-invent database v3.4. *Ecoinvent V3* **2017**, *4*, 1–97.

45. Peters, J.F.; Baumann, M.; Zimmermann, B.; Braun, J.; Weil, M. The environmental impact of Li-Ion batteries and the role of key parameters–A review. *Renew. Sustain. Energy Rev.* **2017**, *67*, 491–506. [CrossRef]

46. Agostini, A.; Belmonte, N.; Masala, A.; Hu, J.; Rizzi, P.; Fichtner, M.; Baricco, M. Role of hydrogen tanks in the life cycle assessment of fuel cell-based auxiliary power units. *Appl. Energy* **2018**, *215*, 1–12. [CrossRef]

47. Hansen, J.B. Solid oxide electrolysis—A key enabling technology for sustainable energy scenarios. *Early Dev.* **2015**, 9–48. [CrossRef] [PubMed]

48. PRé Sustainability. Eco-Indicator 99 Manual for Designers. Available online: https://www.pre-sustainability.com/download/EI99_Manual.pdf (accessed on 2 July 2020).

49. Meyer, L.; Tsatsaronis, G.; Buchgeister, J.; Schebek, L. Exergoenvironmental Analysis for Evaluation of the Environmental Impact of Energy Conversion Systems. *Energy* **2009**, *1*, 75–89. [CrossRef]

50. Mousavi, S.A.; Mehrpooya, M. A comprehensive exergy-based evaluation on cascade absorption- compression refrigeration system for low-temperature applications-exergy, exergoeconomic, and exergoenvironmental assessments. *J. Clean. Prod.* **2020**, *246*, 119005. [CrossRef]

51. Bonforte, G.; Buchgeister, J.; Manfrida, G.; Petela, K. Exergoeconomic and exergoenvironmental analysis of an integrated solar gas turbine/combined cycle power plant. *Energy* **2018**, *156*, 352–359. [CrossRef]

52. José, E.; Cavalcanti, C. Exergoeconomic and exergoenvironmental analyses of an integrated solar combined cycle system. *Renew. Sustain. Energy Rev.* **2017**, *67*, 507–519. [CrossRef]